Post-Shot Data Analysis Tools for Cryogenic Target Shots

Kyle Bensink
Victor Senior High School
Victor, NY
Advisor: Douglas Jacobs-Perkins

Laboratory for Laser Energetics
University of Rochester
Rochester, NY
January 2017

1. Abstract

A series of Matlab programs were developed that can systematically parse and analyze data from multiple cryogenic target positioning control and sensor subsystems on OMEGA. The most involved analysis programs were written to monitor the pressure and leak rate of helium exchange gas within the inner shroud, both of which must be relatively stable in order to tightly control target temperature. Many interrelated factors influence the condition of the deuterium-tritium ice layer within the target as well as target position. Most data sources log data at dissimilar rates - for example, high-speed video logging of target position records rapidly and intermittently in contrast to diagnostic equipment on the moving cryostat transfer cart. As a result, programs that incorporate multiple subsystem data sets needed to correlate time logs in order to parse effectively. As more programs are developed, they will be integrated into the post-shot analysis cycle to generate statistical data, and ultimately will allow subsystem "health" to be closely monitored.

2. Introduction

The University of Rochester Laboratory for Laser Energetics (LLE) is pursuing an effort to demonstrate that it is possible to develop 100 GBar internal target pressure during an inertial confinement target implosion. Physicists believe that 100 GBar performance on OMEGA would scale to ignition if repeated at the National Ignition Facility (NIF).[1] One requirement of the 100 GBar effort is consistent target conditions for each shot. The target position accuracy requirements have been tightened from 10 μm to within 5 μm of the target chamber center, and additionally, the temperature of the target must be maintained within ±5 mK in order to maintain the quality of the deuterium-tritium (DT) ice layer within the target. A variety of interrelated

factors influence these conditions, most of which are currently not regularly monitored and assessed.

The goal of this work was to start developing programs that can help scientists and engineers determine the sensitivity of target performance to operating variables. Once sensitivities are understood, variables with greatest sensitivity will be the focus of improvement efforts.

3. Internal Environment

Figure 1 schematically depicts the construction of the target and the immediate surrounding environment, which are exaggerated for illustrative purposes. The environment is drawn to scale in Figure 2. The target is a small (860 μm diameter) shell filled with a mixture of DT. Part of this mixture is frozen at 19.5 K and forms an ice layer on the inner surface of the shell, surrounding the remaining gas mixture. By nature, tritium is radioactive and produces heat as it decays; thus, the environment surrounding the target needs to conduct excess heat out of the chamber. The target is surrounded by helium exchange gas at a pressure of about 2 torr, which conducts heat away from the target and toward the walls of the inner shroud.

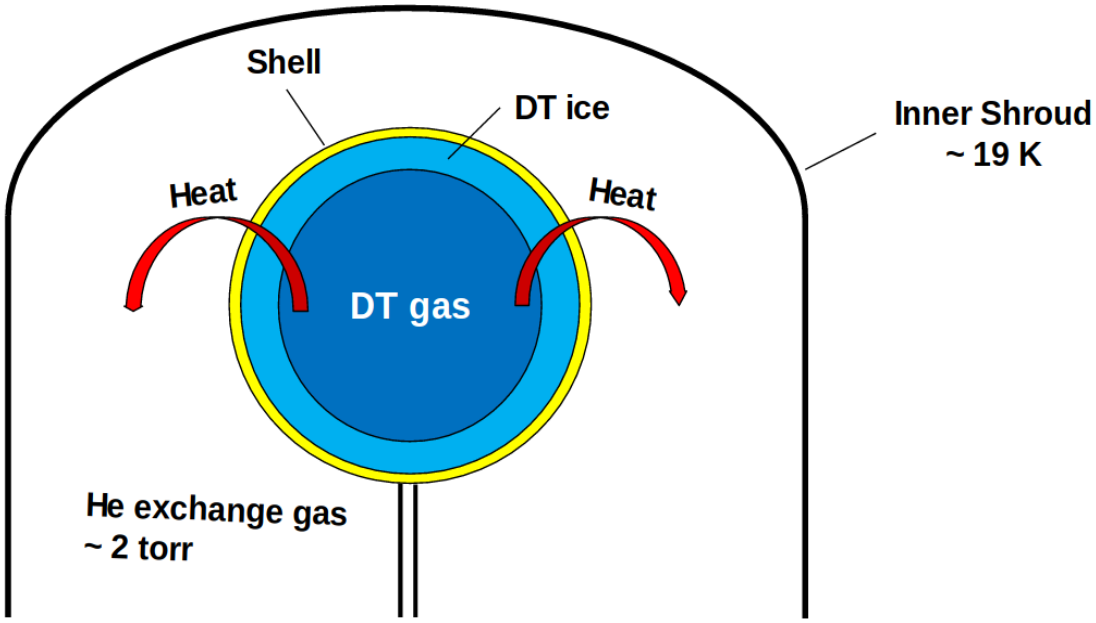

Figure 1. Schematic (not to scale) of target and surrounding environment.
Heat is conducted away by the inner shroud as tritium in the target decays.

3.1 The Shroud

Figure 2 is a computer-aided design (CAD) rendition of the upper section of the moving cryostat transfer cart (MCTC). Shown at top is a gripper mechanism that is attached to a linear induction motor (LIM, not shown). The gripper attaches to the shroud, and the linear motor lifts the shroud clear of the laser beams immediately before the laser fires. The shroud is a 3-part assembly which provides a graduated thermal buffer from the external environment, ensuring that the target remains at a stable temperature. In Figure 2, the shroud is depicted in gray, salmon, and orange portions; the latter of the three is the inner shroud that contains the target.

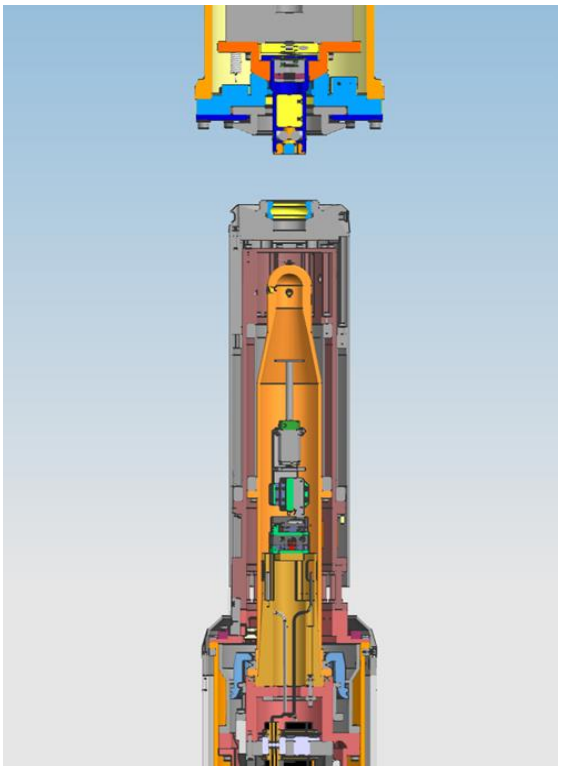

Figure 2. CAD assembly of the upper section of the moving cryostat transfer cart (MCTC) and gripper.
The shroud is shown clamped to the moving cryostat as the gripping mechanism is lowered to the shroud.

3.2 The Shot Cycle

For the majority of the shot cycle, the inner shroud is secured by the parting-joint clamp (shown in blue near the bottom of Fig. 2) applying approximately 500 lbs of force. These clamps maintain a gas-tight seal along the bottom of the shroud, limiting the release of He gas. Small amounts leak out, which is expected, and new gas is introduced to the shroud by a "puffer" circuit intended to maintain the pressure of the He.

When the command is given, the LIM lowers and grips the shroud. At this time, the LIM provides a preload of 250 lb and the inner shroud clamps release. This maintains the seal at the bottom of the shroud. About 5 minutes before the shot is taken, this preload is reduced to 90 lb,

maintaining the seal but less so. As a result, the leak rate of exchange gas increases. One goal of this analysis is to determine if the leak rate is abnormally high, indicating that repairs are necessary before a new target is loaded into the cryostat.

Figure 3 depicts the same assembly as Figure 2, but shortly after the Shroud Pull command is given. The LIM has lifted up the shroud partway, and the clamps at the bottom (shown in sky blue) are fully unclamped. In practice, the movement of the LIM is quite swift in fully uncovering the target; this figure illustrates which pieces are removed in the process.

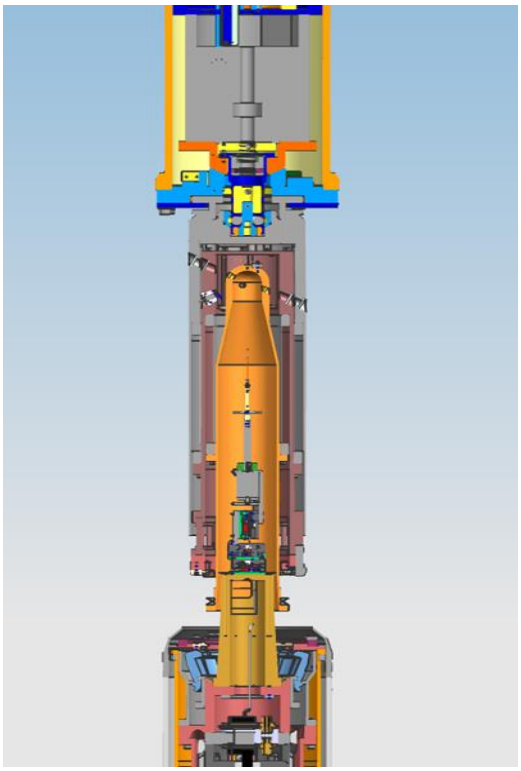

Figure 3. Linear induction motor (LIM) gripped onto shroud.
Clamps are unclamped, and the shroud is being removed.

3.3 Data Sources Used

Every time a test shot is performed on OMEGA, records of all gathered data are stored in LLE's databases. Each data set is saved in the form of a Matlab structure for simple access. Four of the Matlab structures compiled from each shot were used in this work. The MCTC Control Module (MCM) gathers information from the MCTC, providing over 200 unique sets of data. The Linear Motor Control Module (LCM) records from the LIM and contains around 50 data sets. The High-Speed Video (HSV) structure consists of information gathered by the two HSV cameras. Finally, the Cryogenic Shot Command Log (Cryoshot) contains a record of every shot command issued from the control room. These logs consist of three parts: a legend, an array of datetime values, and a substructure which contains the data itself. The MCM and LCM log at a constant rate of 40 Hz, whereas HSV cameras are more variable (see sections 5.1 and 5.2 for more on this difference in logging methods).

4. Characterizing Exchange Gas Leak Rate

Ultimately, the task at hand is to understand the relationship between the load applied to the seal and the leak rate of the He gas, and to determine when an unusual amount of leakage is occurring.

There are four stages of interest when examining the He leak rate: prior to the Shroud Engage; after the shroud is engaged; when the LIM preload is at 250 lb; and when the LIM preload is at 90 lb. Each of these stages has different conditions which characterize its beginning and end. Some of these are data-based, such as the preload reaching a certain value, but others are command-based.

During post-shot data analysis, subroutines parse the requisite sections of data by searching for the starting and ending conditions. The parsed data is then sent through a zero-phase digital filtering function to eliminate unnecessary noise. The filtered data is then searched for local maxima, which correspond to when the puffer circuit introduces new He gas. The distance from maximum to maximum constitutes the period of the gas pressure oscillation, a value which is highly linked to the leak rate itself. For each observed period in the parsed data, the average leak rate is recorded, as well as the maximum and minimum pressure values.

Figure 4 depicts a graph of exchange gas pressure while the LIM preload is at 250 lb (blue) and at 90 lb (yellow). The long, vertical violet line indicates the time at which the command was given to reduce the preload to 90 lb, thus increasing the leak rate. Short multicolored vertical lines in the 250 lb section indicate local maxima identified by the program.

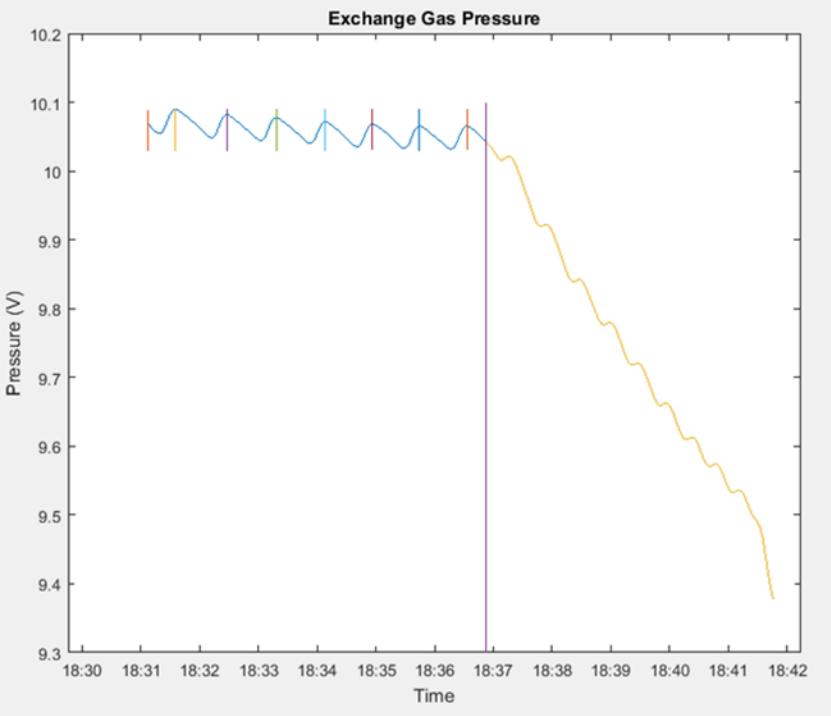

Figure 4. Exchange Gas Pressure during 250 lb and 90 lb Preloads vs. Time (hours:minutes).
Vertical lines divide sections which have been parsed by the program. The leak rate changes abruptly when the preload is reduced from 250 to 90 lb. A periodic pressure increase results from the puffer circuit introducing replacement gas. (Note: for this manometer, a reading of 10 V indicates a pressure of 2 torr).

5. Determining Target Support Stiffness

The target's position is influenced by a variety of factors, one critical factor being the stiffness of the moving cryostat and its associated support structure. When the force applied by the LIM changes, the structure deflects accordingly. In order to have the target precisely positioned after the shroud is removed and these forces are absent, the structure must be characterized in advance so that its deflection is accurately known. The goal of this program is to correlate HSV data with other data to determine the structure's stiffness, and to accurately

predict target location once the shroud is removed. If the stiffness changes over time, it could also be indicative of needed maintenance.

5.1 HSV Cameras

During the shot cycle, the target position is recorded by two HSV cameras. The cameras are positioned nearly orthogonal to each other, so as to accurately determine the target's position in 3-dimensional space. Figure 5 is a graph plotting the target's z-axis position as a function of time. HSV cameras record ensembles of images in ~500 ms bursts at a fixed frame rate between 500-2000 Hz. After each acquisition, analysis is performed and the acquisition/analysis cycle repeats.

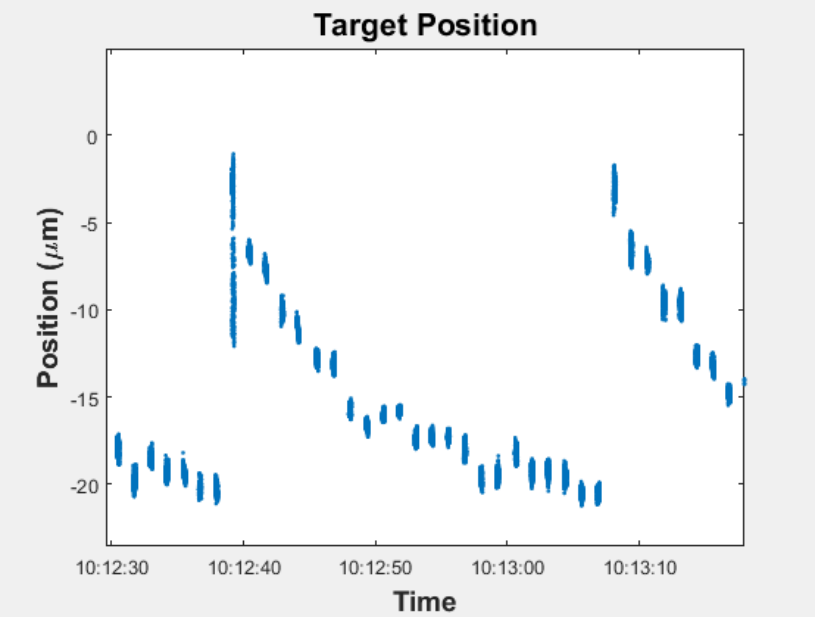

Figure 5. Target position vs. Time (hours:minutes:seconds).
High-speed video images are typically recorded as ensembles at 1-2 kHz frame rate for ~500 ms, then analyzed before the next ensemble is acquired. This leads to the data clusters (above), followed by data gaps. This is in contrast to MCM and LCM data that is sampled at regular intervals.

5.2 Challenges with Aligning HSV to Other Data

In order to properly correlate HSV data with other sources, the timestamps for both data sets need to be equivalent. Data logged from most sources (MCM, LCM, Cryoshot) have timestamps that come from the same clock; however, HSV cameras operate on a different clock that may or may not be synchronized. Figure 6 shows an example of this time mismatch -- for this data set, the HSV timestamps recorded the target moving about 2 seconds before the LIM changed preload.

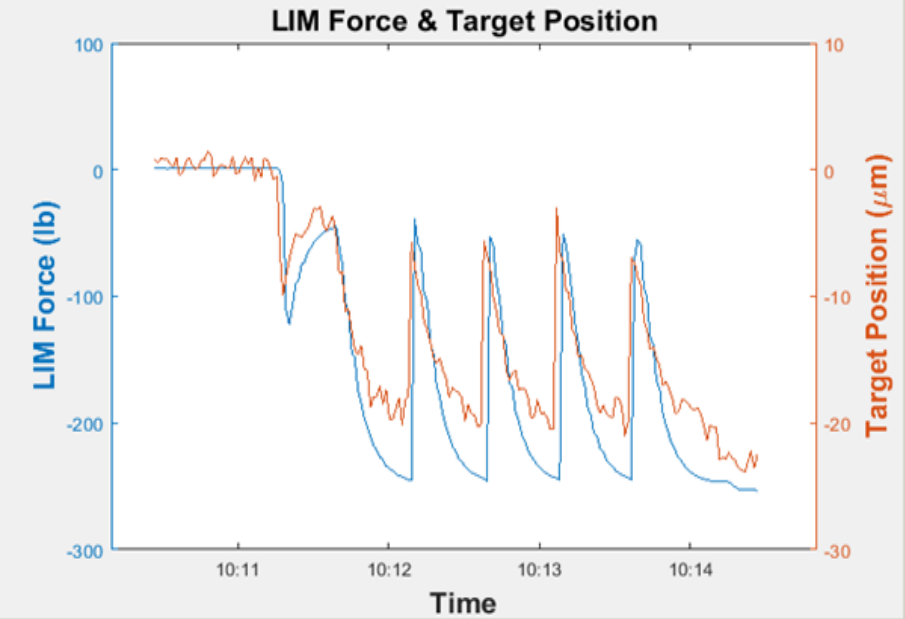

Figure 6. LIM Force and Target Position vs. Time (hours:minutes).
The timestamps for LIM Force and Target Position are not aligned; it appears as if the target moves before the LIM.

Correction of this misalignment is a work in progress. Figure 7 shows data for the same shot as Figure 6, but with the time misalignment manually corrected. Ultimately, the program will use a function to find local maxima in both the LIM Force and HSV data sets, and determine

the average mismatch between their time logs. The time log for HSV will then be altered to remedy the mismatch.

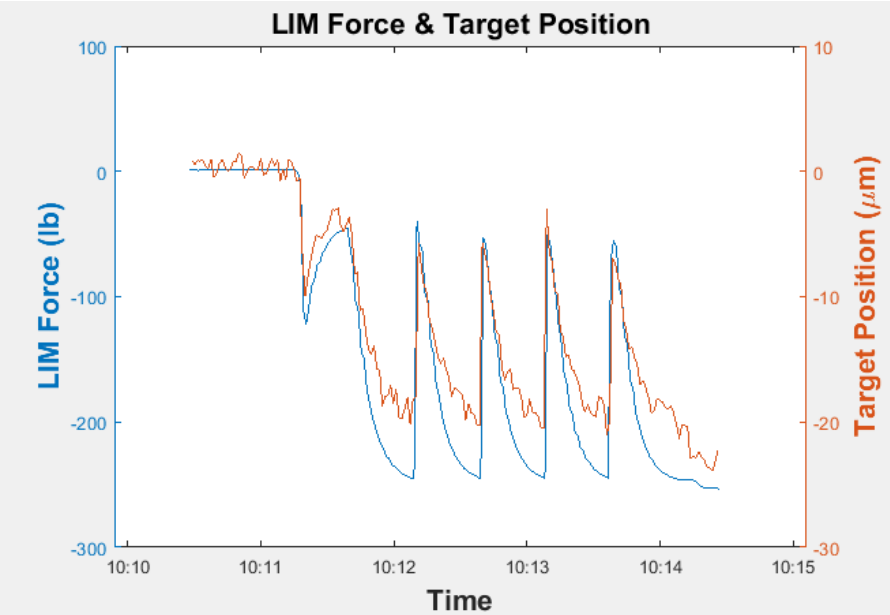

Figure 7. Corrected version of Figure 6.
The HSV camera time log has been manually aligned to match with that of the LIM.

5.3 Determining Target Support Stiffness

HSV target positioning records are correlated with other data sets to ultimately determine how the target reacts to certain changes in its environment. In the case of correlating target position with LIM Force, the goal is to determine the relationship that occurs between the two variables. Figure 8 is a plot of these variables, along with a least-squares regression line (LSRL) to indicate the linear relationship that exists between the two. The trendline predicts that the target will move by 8 μm once the 90 lb LIM preload is removed from the target support structure; this prediction is consistent with prior observations.[2] This correlation will eventually

be performed on each moving cryostat to determine the difference in target support stiffness from one cart to the next.

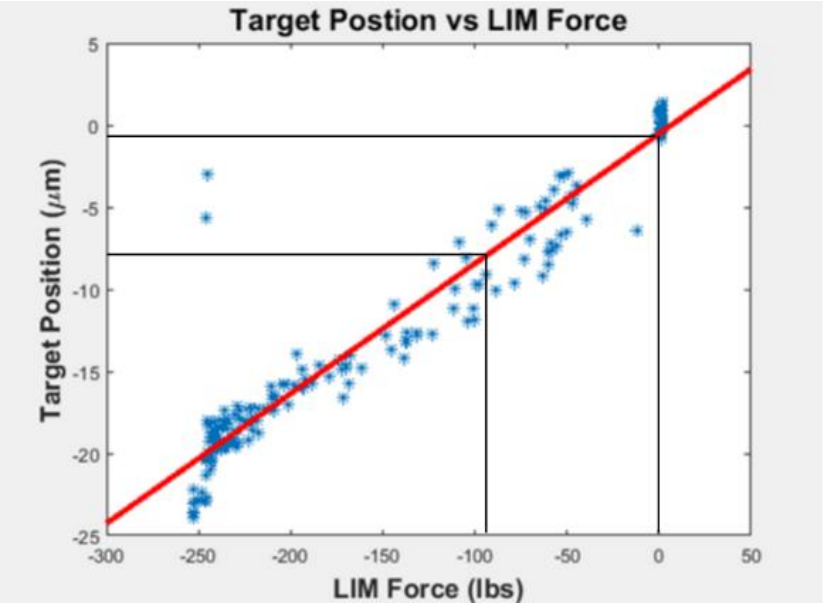

Figure 8. Target Position vs. LIM Force.
The least-squares regression line indicates that the target will move by an average of 8 μm once the 90 lb preload is removed from the support structure.

6. Stored Data

Once data logged from a shot is entered into LLE's databases, the programs developed from this work parse appropriate data from the logs, analyze the results, and save the output back into the databases. Currently, there is no self-acting part in any of the programs that will alert a user when an abnormal shot occurred; one ultimate goal, however, is to determine acceptable thresholds for each statistic.

7. Conclusion

A series of programs were written to systematically parse and analyze data from multiple cryogenic target positioning control and sensor subsystems on OMEGA. The focus of this work was to determine the target's response to certain operating variables, many of which are not currently monitored. Regular assessment of these conditions can lead to quick diagnoses of problems and more consistent shot performance.

One of the most involved programs examines the leak rate of helium exchange gas within the shroud. For each shot, the program parses sections of data, and analyzes the leak rate under each of four conditions. Other values of interest are recorded as well, such as the period of oscillation and the range of pressure values. These findings are recorded in the database for later reference.

The other main program involves correlating target positioning imaging with the LIM force applied to the shroud, so as to determine the stiffness of the target support structure. Since HSV timestamps are not always aligned with other sources, a sub-function is being written to correct the average error in the HSV timestamp. This allows for stronger correlation between data, and a better prediction of where the target will be located when the shot is fired.

8. Acknowledgements

I thank Dr. Craxton for managing this program, which provides students like myself with an opportunity to work in a research-based environment. I also thank Jeffrey Ulreich for providing the CAD images in this report. Finally, I thank Dr. Jacobs-Perkins for his endless guidance and patience in working with me on this project.

9. References

[1] "Implosion Dynamics in Direct-Drive Experiments." *LLE Review 139*, pp. 158-159 (2014).

[2] S. X. Hu, V. N. Goncharov, P. B. Radha, J. A. Marozas, S. Skupsky, T. R. Boehly, T. C. Sangster, D. D. Meyerhofer, and R. L. McCrory, *Phys. Plasmas 17*, 102706 (2010).